Published in final edited form as:
J Biomech. 2014 September 22; 47(12): 3115–3119. doi:10.1016/j.jbiomech.2014.06.026.

Bioinjection Treatment: Effects of Post-Injection Residual Stress on Left Ventricular Wall Stress

Lik Chuan Lee[7], **Samuel T. Wall**[4], **Martin Genet**[1,2,3,5], **Andy Hinson**[6], and **Julius M. Guccione**[1,2,3]

[1]Department of Surgery, University of California, San Francisco, CA

[2]Bioengineering, University of California, San Francisco, CA

[3]Medicine, University of California, San Francisco, CA

[4]Simula Research Laboratory, Oslo, Norway

[5]Marie-Curie Outgoing fellow

[6]Lonestar Heart Inc

[7]Department of Mechanical Engineering, Michigan State University, MI, USA

Abstract

Injection of biomaterials into diseased myocardium has been associated with decreased myofiber stress, restored left ventricular (LV) geometry and improved LV function. However, its exact mechanism(s) of action remained unclear. In this work, we present the first patient-specific computational model of biomaterial injection that accounts for the possibility of residual strain and stress introduced by this treatment. We show that the presence of residual stress can create more heterogeneous regional myofiber stress and strain fields. Our simulation results show that the treatment generates low stress and stretch areas between injection sites, and high stress and stretch areas between the injections and both the endocardium and epicardium. Globally, these local changes are translated into an increase in average myofiber stress and its standard deviation (from 6.9 ± 4.6 to 11.2 ± 48.8 kPa and 30 ± 15 to 35.1 ± 50.9 kPa at end-diastole and end-systole, respectively). We also show that the myofiber stress field is sensitive to the void-to-injection size ratio – for a constant void size, the myofiber stress field became less heterogeneous with decreasing injection volume. These results suggest that the residual stress and strain possibly generated by biomaterial injection treatment can have large effects on the regional myocardial stress and strain fields, which may be important in the remodeling process.

Corresponding Author: Lik Chuan, Lee, PhD, Department of Mechanical Engineering, Michigan State University, 2445 Engineering Building, East Lansing, MI 48824-1226, USA, lclee@egr.msu.edu.

Potential Conflict of Interest: Mr. Hinson is an employee of LoneStar Heart, Inc.

Keywords

Congestive heart failure; biomaterial injection; left ventricular wall stress; mathematical modeling; magnetic resonance imaging

1. Introduction

Injection of materials into the myocardium as a treatment for heart diseases has generated considerable interest over recent years. The injection of biomaterials, which range from biological materials e.g., Alginate (Landa et al., 2008) and Fibrin (Christman et al., 2004), to synthetic hydrogels (Jiang et al., 2009), have shown positive outcomes in animal studies. Recently, significant reverse remodeling – 50% reduction in end-diastolic volume (EDV) and end-systolic volume (ESV) – in patients suffering from dilated cardiomyopathy was observed as early as 3 months after injection of Algiysl-LVR™ (a calcium-sodium alginate hydrogel) and Coronary Artery Bypass Grafting (Lee et al., 2013a).

Despite these favorable outcomes, the exact mechanism(s) of action of the injection treatment remain(s) unclear. While the treatment's primary rationale is to provide support to the diseased myocardium to reduce ventricular wall stress (widely believed to be responsible for adverse cardiac remodeling), there are also suggestions that these injected biomaterials can create a “healthier micro-environment through stress shielding” that increases capillary and arteriole densities (Nelson et al., 2011). Thus, the effects of this treatment need to be better understood, especially because of its potential as an effective treatment for heart diseases.

Computational modeling has been used to better understand the effects of injecting material into the myocardium (Kortsmit et al., 2012; Wall et al., 2006; Wenk et al., 2009). These modeling studies generally support the primary rationale of the injection treatment: helping to provide support to the myocardium through thickening of the ventricular wall to reduce ventricular wall stress. However, these studies did not include the possible effects of residual stress that could occur when injections are introduced into the myocardium. The effects of residual stresses that were imparted to the myocardium after implantation of other treatment devices into the heart has been considered in other analyses (Carrick et al., 2012; Lee et al., 2014).

Injectable biomaterials usually begin in a viscous liquid that solidifies though chemical changes *in situ* to form a solid hydrogel (Christman et al., 2004; Lee et al., 2013b). When injected, these liquids are forced into the myocardium, creating new space to accommodate the bleb of material. As such, residual stress can be introduced during this process, especially when the void that accommodates the injection has an initial volume smaller than the injected volume itself. Although the myocardial extracellular space (∼ 24% of the tissue space) consists of about 6% “empty” space devoid of any structural components (Frank and Langer, 1974) - about 2.7 ml for a left ventricular (LV) wall volume of 190 ml in the patient-specific model described here, they are interspersed within the myocardium and the local “empty” space is substantially smaller. Hence, it is likely that residual stress could be

present when the injection volume ~ 0.3 ml (Lee et al., 2013a) is greater than the local "empty" or void space.

The primary aims of this paper are twofold: first, to describe a methodology to model the effects of post-injection residual stress, and second, to highlight the possible effects of residual stress on local myofiber stress and stretch fields.

2. Methods and Results

2.1 Finite element model of the LV

A patient-specific finite element (FE) model of the LV was constructed based on the baseline magnetic resonance (MR) images of patient 1 described in Lee et al. (2013a). The patient was diagnosed with NYHA class III heart failure and had ischemic cardiomyopathy, hypertension, hyperlipidemia and renal insufficiency. The LV was modeled using 110,976 trilinear hexahedral elements and the FE mesh was graded so that its mesh density was 4 times higher at the mid-LV (where the injections are located) (Figure 1a).

Nearly incompressible and transversely isotropic hyperelastic material laws for the passive (Guccione et al., 1991) and active myocardium (Guccione et al., 1993) were used to model the mechanical behavior of the LV during a cardiac cycle. The material passive stiffness (C) and the tissue contractility (T_{max}) were chosen so that the predicted LV volumes (without injection) matched the corresponding EDV (197ml) and ESV (122ml) measured from MR images. All other parameters had values equal to those used in large animal studies (Sun et al., 2009) and human study (Wenk et al., 2012).

Local fiber direction was defined on the local tangent plane by prescribing a fiber angle taken with respect to the local circumferential vector running counterclockwise when viewed in the base-to-apex direction. In the entire LV, the fiber angle varied linearly from the endocardium (60°) to the epicardium (-60°) (Streeter et al., 1969) (Figure 1b). The epicardial-base edge was fixed, whereas the base displacement was constrained in the out-of-plane direction.

Three simulation cases, namely, BASELINE, RESIDUAL and NO-RESIDUAL were performed. BASELINE was defined to be the case before injections. RESIDUAL and NO-RESIDUAL corresponded to the post-injection cases with and without the effects of residual stress, respectively.

2.2 Modeling injections into the LV

The LV wall was meshed with spherical voids at the mid-LV (halfway between the base and the apex) and the voids were filled with hexahedral elements. The finite element meshes of the voids and the LV wall have matching nodes at their common interface. There were a total of 12 voids, each with an arbitrarily prescribed radius of 1mm (Figure 1c).

To model the effects arising from post-injection residual stress (RESIDUAL), the hexahedral elements in the void were first prescribed with a dummy material law and a spherical displacement field was then imposed to dilate each void to an arbitrary prescribed

injection volume of 0.02 ml. Thereafter, stresses were initialized to zero in the elements defining the void and these elements were prescribed with a material law describing the hydrogel injections. In other words, the elements within the void now define the injected hydrogel. The hydrogel injections were modeled using nearly incompressible Mooney-Rivlin material law with previously obtained parameters (Wenk et al., 2009) from alginate experiments. Then, the spherical displacement field was removed to allow the injections and the LV to deform until a force-equilibrium was reached (Figure 1d). This resultant configuration is defined to be the unloaded (but not stress-free) configuration. In NO-RESIDUAL, stresses of both the injections and LV wall were initialized to zero from the unloaded configuration of the RESIDUAL case.

End-diastole (ED) and end-systole (ES) were simulated in all 3 cases by imposing a pressure boundary condition of 20 mm Hg and 125 mm Hg at the endocardial wall in the unloaded configuration, respectively. All simulations were performed using LS-DYNA (Livermore Software Technology Corporation, Livermore, CA) with the passive and active myocardial material law implemented as a user-defined material subroutine.

2.3 Effect on Global Stretch and Stress in Myofiber and Cross-myofiber directions

Stretch and stress in both the myofiber and cross-myofiber directions were averaged over the entire LV at ED and ES for BASELINE, RESIDUAL and NO-RESIDUAL (Table 1). The average stress and stretch (at ES and ED) were not very different between BASELINE and NO-RESIDUAL in both the myofiber and cross-myofiber directions. However, the average ED myofiber stress of RESIDUAL (11.2 ± 48.8 kPa) was nearly twice as large as that of BASELINE (6.9 ± 4.6 kPa), whereas the average ES myofiber stress of RESIDUAL (35.1 ± 50.9 kPa) was 17% higher than that of BASELINE (30 ± 15 kPa). Similar trend was also observed for the cross-myofiber stress of RESIDUAL, which was higher than BASELINE. The average ED and ES stretch of RESIDUAL was not very different from that of BASELINE in both the myofiber and cross-myofiber directions. In general, both ES and ED stress and stretch in RESIDUAL had larger values of standard deviation than BASELINE and NO-RESIDUAL.

2.4 Effect on Local Myofiber Stretch and Stress

The substantially larger standard deviation found in RESIDUAL suggests that the myofiber stress and stretch were more heterogeneous than the other 2 cases. Moreover, the significantly larger change in fiber stress than in fiber stretch indicates that out-of-fiber-direction tensions and shear-stress components must be activated.

Closer inspection of the myofiber stretch and stress fields reveals an organized pattern in the injection region, particularly in RESIDUAL when compared to NO-RESIDUAL (Figures 2 and 3). In RESIDUAL, the myofiber stretch was substantially decreased and was less than unity at the mid-wall between injections at both ED and ES. At ES, the myofiber stretch was elevated in the transmural direction between the injections and the endocardium, as well as between the injections and the epicardium. The ES myofiber stress field displayed similar pattern as that of the ES myofiber stretch. Contrastingly, ED myofiber stress did not decrease substantially between the injections that were located at the mid-wall and was

elevated in the transmural direction between the injections and both the epicardium and the endocardium.

Without residual stress (NO-RESIDUAL), the myofiber stretch and stress fields at the injection region were largely similar to those in BASELINE, with the exception that the ED and ES myofiber stress between injections was slightly lower than in BASELINE (Figure 3).

2.5 Effect of void-to-injection size ratio on myofiber stress

The myofiber stress is also sensitive to the void-to-injection size ratio. By keeping the void size constant, both global ES and ED average myofiber stress decreases with decreasing injection volume (Figure 4a). In addition, the standard deviation of the myofiber stress also decreased substantially with decreasing injection volume and approaches the values in NO-RESIDUAL. Correspondingly, the myofiber stress field became more homogeneous near the injection sites (Figure 4b).

2.6 Effect on ventricular volume

The injections had little effects on both EDV and ESV in RESIDUAL and NO-RESIDUAL. Only in RESIDUAL was the EDV slightly smaller (198 ml) than BASELINE (201ml).

3. Discussions

3.1 Myofiber stretch and stress heterogeneity

Although the inclusion of residual stress in our simulations led to elevated global averaged myofiber stress when material was added to the myocardium, this increase was associated with a greater increase in its standard deviation due to a resulting complex pattern of loading and unloading. As such, the principal finding of our simulation is that residual stress can dramatically increase heterogeneity of the myofiber stretch and stress fields, and may not lead to an average decrease in wall stress seen in previous studies. Specifically, the presence of residual stress produced a regular pattern of low myofiber stretch between injections in the LV mid-wall, and high myofiber stretch extending from the injections towards the endocardium and epicardium (Figures 2 and 3). The less than unity myofiber stretch between the injections at ED and ES implies that the mid-wall myofibers were compressed or “unloaded” throughout the cardiac cycle. This result can be explained by considering the myofiber orientation across the LV wall (Figure 1b). Because myofibers are oriented circumferentially at the mid-wall, they were compressed by the expanding voids that accommodated the injections. Contrastingly, the expanding voids also stretch the obliquely-oriented sub-endocardial and sub-epicardial myofibers. Given that myofiber strain has also been hypothesized as a regulator of myocardial growth (Omens, 1998), the heterogeneous myofiber stretch field near the injections may have direct implication on the remodeling process.

The transmurally elongated ellipsoidal shape of the injection in the unloaded configuration (Figure 1b) is a consequence of (a) our assumption of a spherical void and (b) the anisotropic material behavior of the myocardium. Given that the LV wall is stiffest in the myofiber direction in our material model (Guccione et al., 1991), and the myofiber runs

circumferentially at the LV mid-wall, the compressive force acting on the initially spherical injections is therefore greatest along the circumferential direction of the LV wall. As a result, the injections were compressed in the circumferential direction of the LV wall. To preserve the injection volumes (as hydrogel is incompressible), the injections became elongated in the transmural direction.

Given that the contractile force generated by the myocytes is directly related to the sarcomere length (Guccione et al., 1993; ter Keurs et al., 1980), the decrease in mid-wall sarcomere length (reflected by a decrease in myofiber stretch) should, in principle, decrease the contractile force generated in that region. This effect is apparent in Figure 3, which shows a reduced mid-wall ES myofiber stress in RESIDUAL.

Another important effect of the injection-induced residual stress is evidenced by the fact that myofiber stretch is much less affected than myofiber stress at ED. This result is possible only if stress components transverse to the fiber direction are changed to balance the change in myofiber stress. Consequently, the myocardium supports a very different state of stress: one with potentially high shear components, and tension in the direction normal to the fiber direction (Table 1). If cross-fiber sensor located at the Z-disk is indeed present, as suggested by Russell et al. (2010), this difference (in stress state) may also potentially play a critical role in affecting tissue growth.

Last, it must be pointed out that the total prescribed injection volume of 0.24 ml is relatively small when compared to other computational models of injection treatment which have larger injection volumes e.g. ∼ 5ml (Wall et al., 2006; Wenk et al., 2009) and ∼ 9.4ml (Kortsmit et al., 2012). We did not increase the injection volume because doing so would lead to a highly distorted mesh near the injections, which would cause numerical instability. As a result, without the presence of residual stresses (NO-RESIDUAL), the injections have little effect on the global averaged myofiber stress and stretch as seen in Table 1.

3.3 Ventricular volume change

The little effect on EDV and ESV in RESIDUAL and NON-RESIDUAL is due to the small amount of injection prescribed in our models as discussed above. In other computational models of injection treatment (Wall et al., 2006; Wenk et al., 2009), a larger injection volume produced a greater effect on EDV and ESV.

3.4 Limitations

The key limitation of this model is the assumption of spherical voids that have a radius of 1mm in the myocardium, which of course, is an idealization. The void is most likely not perfectly spherical and uniform in size. Moreover, the inflation of voids during the injection process could be further complicated by any fracture planes the hydrogel could force open during injection. If all these complications are present, the resultant shape of the injection would most likely be different from our model prediction. For example, the injection of Methacrylated Hyaluronic Acid in normal ovine heart was found to be elongated circumferentially in the myofiber direction (Kichula et al., 2013) as opposed to our model's prediction that the injection is elongated in the transmural direction. Since residual stress can only be present if there is a misfit between the injection and the void, the degree of residual

stress is sensitive to the void-to-injection size ratio (Figure 4) and how the void deforms and expands with injection. Experimental studies providing information on the shape and sizes of the myocardial voids could be performed in the future so that the degree and effects of residual stress can be better quantified.

3.5 Summary

In conclusion, we have described the first model that incorporates the effects of residual stress introduced by the injection of materials into the LV. Our results show that the stress and stretch fields near the injection region became more heterogeneous, whereby myofibers between the injections were unloaded and myofibers between the injections and both endocardium and epicardium were pre-stretched. These results are preliminary and models that incorporate more detailed microstructural information are needed to shed light on the possible role of residual stress in the reported therapeutic effects associated with the injection treatment.

Acknowledgments

This study was supported by National Heart, Lung, and Blood Institute Grants R01-HL-077921, R01-HL-118627 (to J. M. Guccione), and by a Marie-Curie International Outgoing Fellowship within the 7th European Community Framework Programme (M. Genet). We would like to thank Pamela Derish in Department of Surgery at UCSF for proofing the manuscript.

References

Carrick R, Ge L, Lee LC, Zhang Z, Mishra R, Axel L, Guccione JM, Grossi Ea, Ratcliffe MB. Patient-specific finite element-based analysis of ventricular myofiber stress after Coapsys: importance of residual stress. Ann Thorac Surg. 2012; 93:1964–71. [PubMed: 22560323]

Christman KL, Fok HH, Sievers RE, Fang Q, Lee RJ. Fibrin glue alone and skeletal myoblasts in a fibrin scaffold preserve cardiac function after myocardial infarction. Tissue Eng. 2004; 10:403–9. [PubMed: 15165457]

Frank JS, Langer Ga. The myocardial interstitium: its structure and its role in ionic exchange. J Cell Biol. 1974; 60:586–601. [PubMed: 4824287]

Guccione JM, McCulloch AD, Waldman LK. Passive material properties of intact ventricular myocardium determined from a cylindrical model. J Biomech Eng. 1991; 113:42–55. [PubMed: 2020175]

Guccione JM, Waldman LK, McCulloch AD. Mechanics of active contraction in cardiac muscle: part II-cylindrical models of the systolic left ventricle. J Biomech Eng. 1993; 115:82–90. [PubMed: 8445902]

Jiang XJ, Wang T, Li XY, Wu DQ, Zheng Z Bin, Zhang JF, Chen JL, Peng B, Jiang H, Huang C, Zhang XZ. Injection of a novel synthetic hydrogel preserves left ventricle function after myocardial infarction. J Biomed Mater Res A. 2009; 90:472–7. [PubMed: 18546187]

Kichula ET, Wang H, Dorsey SM, Szczesny SE, Elliott DM, Burdick Ja, Wenk JF. Experimental and Computational Investigation of Altered Mechanical Properties in Myocardium after Hydrogel Injection. Ann Biomed Eng. 2013

Kortsmit J, Davies NH, Miller R, Macadangdang JR, Zilla P, Franz T. The effect of hydrogel injection on cardiac function and myocardial mechanics in a computational post-infarction model. Comput Methods Biomech Biomed Engin. 2012

Landa N, Miller L, Feinberg MS, Holbova R, Shachar M, Freeman I, Cohen S, Leor J. Effect of injectable alginate implant on cardiac remodeling and function after recent and old infarcts in rat. Circulation. 2008; 117:1388–96. [PubMed: 18316487]

Lee LC, Ge L, Zhang Z, Pease M, Nikolic SD, Mishra R, Ratcliffe MB, Guccione JM. Patient-specific finite element modeling of the Cardiokinetix Parachute(®) device: effects on left ventricular wall stress and function. Med Biol Eng Comput. 2014

Lee LC, Wall ST, Klepach D, Ge L, Zhang Z, Lee RJ, Hinson A, Gorman JH, Gorman RC, Guccione JM. Algisyl-LVR™ with coronary artery bypass grafting reduces left ventricular wall stress and improves function in the failing human heart. Int J Cardiol. 2013a; 168:2022–2028. [PubMed: 23394895]

Lee LC, Zhihong Z, Hinson A, Guccione JM. Reduction in left ventricular wall stress and improvement in function in failing hearts using Algisyl-LVR. J Vis Exp. 2013b:1–6.

Nelson DM, Ma Z, Fujimoto KL, Hashizume R, Wagner WR. Intra-myocardial biomaterial injection therapy in the treatment of heart failure: Materials, outcomes and challenges. Acta Biomater. 2011; 7:1–15. [PubMed: 20619368]

Omens JH. Stress and strain as regulators of myocardial growth. Prog Biophys Mol Biol. 1998; 69:559–72. [PubMed: 9785956]

Russell B, Curtis MW, Koshman YE, Samarel AM. Mechanical stress-induced sarcomere assembly for cardiac muscle growth in length and width. J Mol Cell Cardiol. 2010; 48:817–23. [PubMed: 20188736]

Streeter DD, Spotnitz HM, Patel DP, Ross J, Sonnenblick EH. Fiber orientation in the canine left ventricle during diastole and systole. Circ Res. 1969; 24:339–47. [PubMed: 5766515]

Sun K, Stander N, Jhun CS, Zhang Z, Suzuki T, Wang GY, Saeed M, Wallace AW, Tseng EE, Baker AJ, Saloner D, Einstein DR, Ratcliffe MB, Guccione JM. A computationally efficient formal optimization of regional myocardial contractility in a sheep with left ventricular aneurysm. J Biomech Eng. 2009; 131:111001. [PubMed: 20016753]

Ter Keurs HE, Rijnsburger WH, van Heuningen R, Nagelsmit MJ. Tension development and sarcomere length in rat cardiac trabeculae. Evidence of length-dependent activation. Circ Res. 1980; 46:703–714. [PubMed: 7363419]

Wall ST, Walker JC, Healy KE, Ratcliffe MB, Guccione JM. Theoretical impact of the injection of material into the myocardium: a finite element model simulation. Circulation. 2006; 114:2627–35. [PubMed: 17130342]

Wenk JF, Klepach D, Lee LC, Zhang Z, Ge L, Tseng EE, Martin A, Kozerke S, Gorman JH, Gorman RC, Guccione JM. First evidence of depressed contractility in the border zone of a human myocardial infarction. Ann Thorac Surg. 2012; 93:1188–93. [PubMed: 22326127]

Wenk JF, Wall ST, Peterson RC, Helgerson SL, Sabbah HN, Burger M, Stander N, Ratcliffe MB, Guccione JM. A method for automatically optimizing medical devices for treating heart failure: designing polymeric injection patterns. J Biomech Eng. 2009; 131:121011. [PubMed: 20524734]

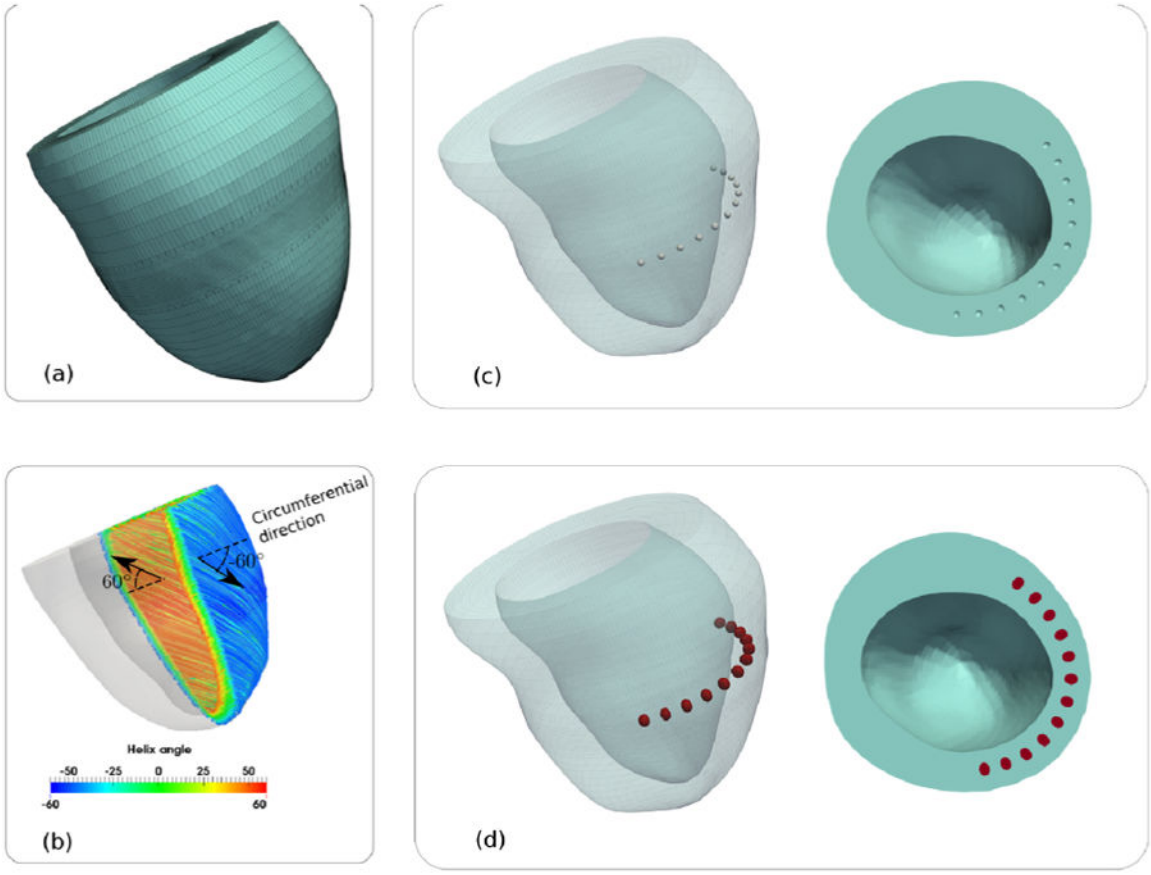

Figure 1.

(a): Finite element mesh of the patient-specific LV. (b): Transmural variation of the myofiber orientation. Left ventricular mesh with (c): 12 spherical voids each having a 1mm radius and (d): injections (red) filling up the void spaces. Notice that the injections are no longer spherical and are slightly elongated transmurally.

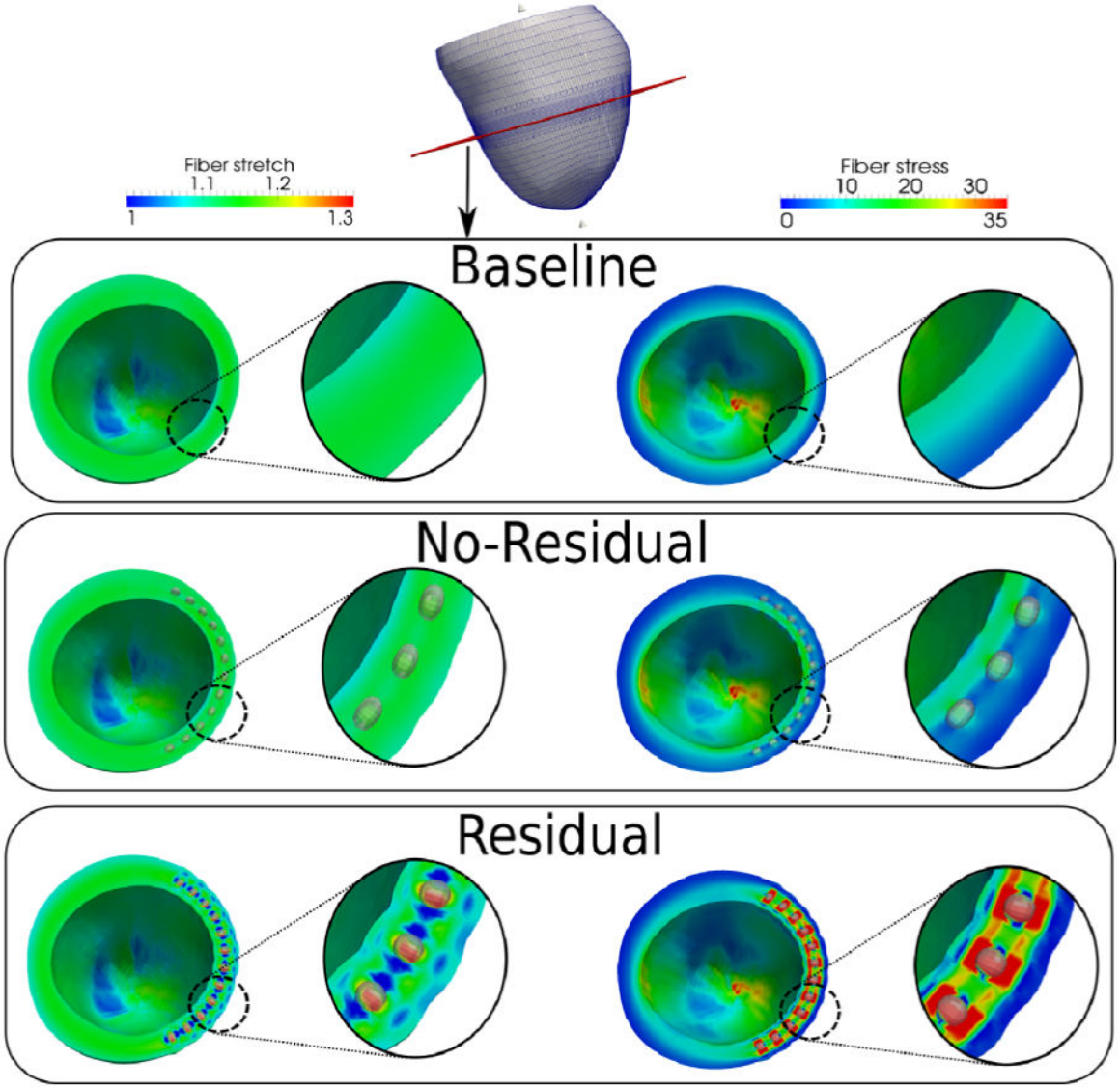

Figure 2.

Comparison of fiber stretch and stress for the baseline, no-residual and residual cases at end-of-diastole. Cutting plane is shown in red at the top picture. Unit of fiber stress is kPa.

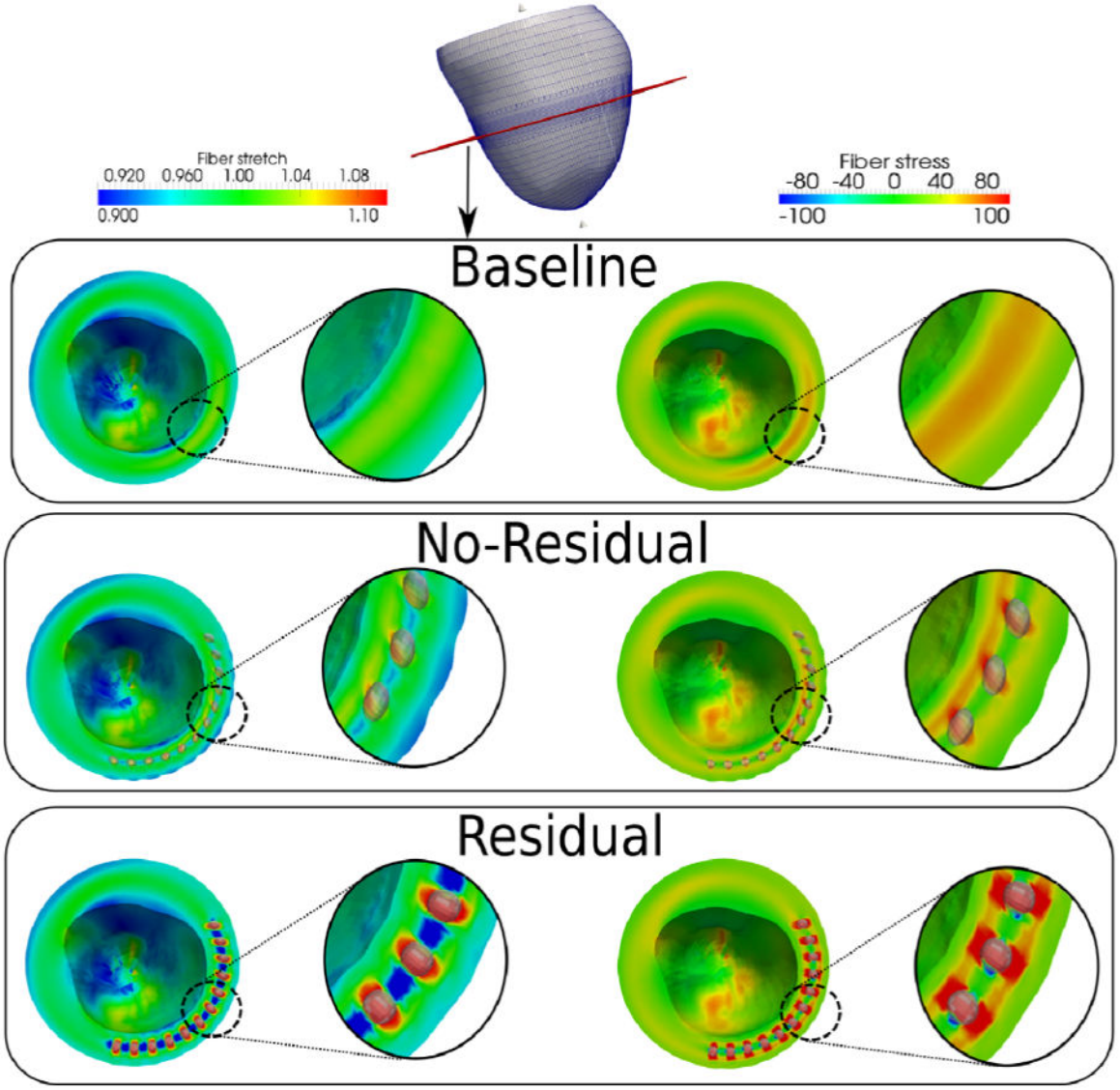

Figure 3.

Comparison of fiber stretch and stress for the baseline, no-residual and residual cases at end-of-systole Cutting plane is shown in red at the top picture. Arrow in the residual case indicates the reduced mid-wall end-systolic myofiber stress. Unit of fiber stress is kPa.

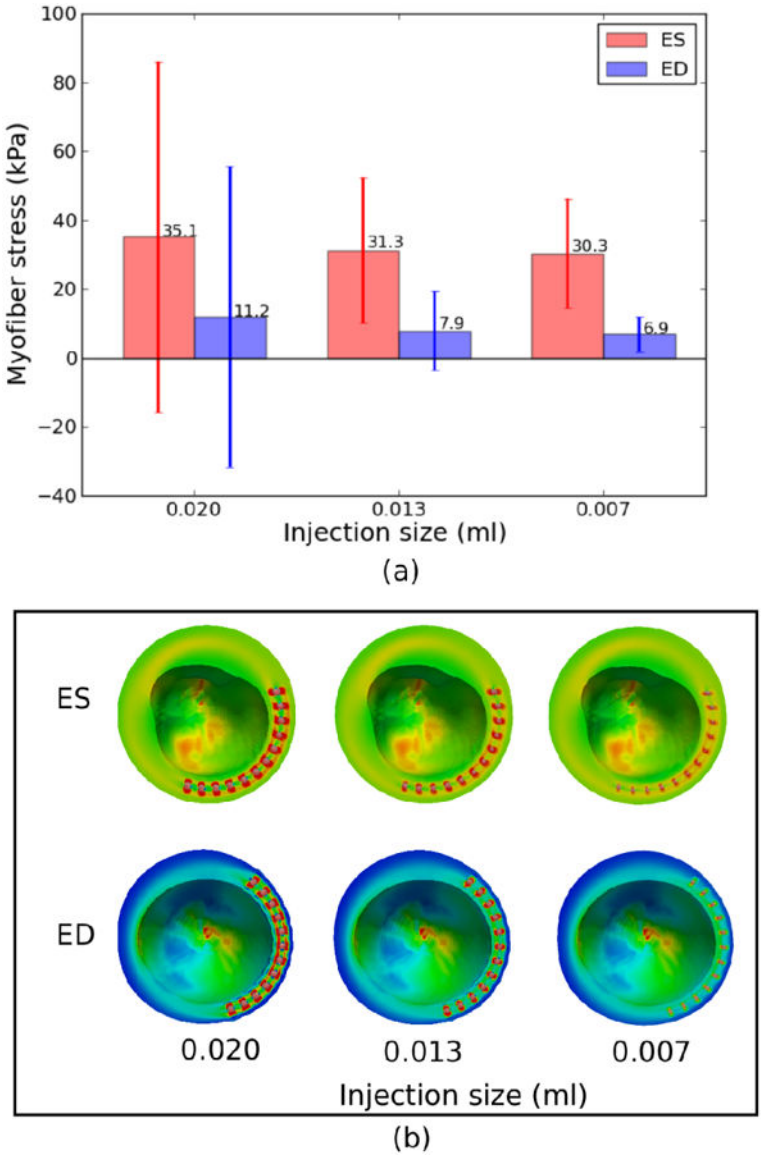

Figure 4.

Effects of injection size (with constant void size) on (a) global myofiber stress and (b) regional myofiber stress near the injection sites. Mean values of myofiber stress are given on top of each bar in (a). Refer to Fig. 2 and 3's legend for ED and ES regional myofiber stress in (b), respectively.

Table 1

Myofiber and cross-myofiber stretch and stress (average ± standard deviation at end-diastole (ED) and end-systole (ES). Refer to text description of BASELINE, RESIDUAL and NO-RESIDUAL.

		BASELINE	RESIDUAL	NO-RESIDUAL
Myofiber stretch	ED	1.12 ± 0.02	1.11 ± 0.04	1.12 ± 0.02
	ES	0.97 ± 0.03	0.97 ± 0.04	0.97 ± 0.03
Cross Myofiber stretch	ED	1.12 ± 0.05	1.11± 0.06	1.12 ± 0.04
	ES	1.00 ± 0.06	1.01 ± 0.07	1.01 ± 0.07
Myofiber stress (kPa)	ED	6.9 ± 4.6	11.2 ± 48.8	6.7 ± 4.6
	ES	30 ± 15	35.1 ± 50.9	30 ± 15
Cross Myofiber stress (kPa)	ED	3.9 ± 3.8	8.1 ± 50.1	3.8 ± 3.8
	ES	8.1 ± 8.2	13.4 ± 57.9	8.1 ± 8.3